

UNCLASSIFIED

NACA

## RESEARCH MEMORANDUM

AERODYNAMIC CHARACTERISTICS AT SUBSONIC AND SUPERSONIC

MACH NUMBERS OF A THIN TRIANGULAR WING OF ASPECT

RATIO 2. II - MAXIMUM THICKNESS AT MIDCHORD

By Harold J. Walker and Robert E. Berggren

Ames Aeronautical Laboratory  
Moffett Field, Calif.

CLASSIFICATION CANCELLED

Author: *Block R 7 2398* Date *8/18/54*

CLASSIFIED DOCUMENT

This document contains classified information affecting the National Defense of the United States within the meaning of the Espionage Act, USC 8042 and 8043. Its transmission or the revelation of its contents in any manner to an unauthorized person is prohibited by law. Information so classified may be imparted only to persons in the military and naval service of the United States, appropriate civilian officers and employees of the Federal Government who have a legitimate interest therein, and to United States citizens of known loyalty and discretion who of necessity must be informed thereof.

By *7/14/54* 9/7/54 SeeNATIONAL ADVISORY COMMITTEE  
FOR AERONAUTICSWASHINGTON  
December 3, 1948

UNCLASSIFIED



UNCLASSIFIED

## NATIONAL ADVISORY COMMITTEE FOR AERONAUTICS

RESEARCH MEMORANDUMAERODYNAMIC CHARACTERISTICS AT SUBSONIC AND SUPERSONIC MACH  
NUMBERS OF A THIN TRIANGULAR WING OF ASPECT RATIO 2.

## II - MAXIMUM THICKNESS AT MIDCHORD

By Harold J. Walker and Robert E. Berggren

## SUMMARY

The lift, drag, and pitching-moment characteristics of a triangular wing, having an aspect ratio of 2 and a symmetrical double-wedge profile of 5-percent-chord maximum thickness at midchord, have been evaluated from wind-tunnel tests at Mach numbers from 0.50 to 0.975 and from 1.09 to 1.49 and at Reynolds numbers ranging from 0.67 to 0.85 million.

The lift, drag, and pitching-moment coefficients of the triangular wing with a leading-edge sweepback of approximately  $63^\circ$  did not exhibit the irregular variations with Mach number at high subsonic and low supersonic Mach numbers that are characteristic of unswept wings. The lift-curve slope increased steadily with Mach number below unity and declined slowly beyond the Mach number of 1.13. A substantial rise in the minimum drag coefficient occurred between Mach numbers of 0.95 and 1.20 with an associated reduction in the maximum lift-drag ratio. The aerodynamic center shifted rearward toward the centroid of area of the wing with increasing Mach number below 0.975; whereas above 1.09 it coincided with the centroid.

To show the effect of a change in location of maximum thickness, a comparison is made between the characteristics of the above wing with those of a wing of identical plan form having the maximum thickness located at 20 percent of the chord. Moving the point of maximum thickness from 20 to 50 percent of the chord gave rise to little or no measurable change in the lift, drag, and pitching-moment characteristics at subsonic Mach numbers. However, at the lower supersonic Mach numbers, lower lift-curve slopes, larger minimum drag coefficients, and smaller maximum lift-drag ratios were exhibited by the wing with maximum thickness at the midchord location, although the differences in each case were small.

██████████

UNCLASSIFIED

## INTRODUCTION

The wing of triangular plan form has been considered from both theoretical and applied standpoints as a practical lifting surface for transonic and supersonic aircraft. The aerodynamic characteristics of this wing can be predicted for moderately high subsonic and for supersonic Mach numbers by the methods of references 1, 2, and 3; however, at present no reliable methods for calculating these characteristics in the Mach number range near unity are available. Some indication of the extent to which the experimental and calculated characteristics diverge near unity has been shown in reference 4, wherein the lift, drag, and pitching-moment characteristics of a low-aspect-ratio triangular wing with the maximum-thickness point at 20 percent of the chord were determined experimentally. In the present investigation these characteristics have been measured at high subsonic and low supersonic Mach numbers for a triangular wing differing from that of reference 4 only in the location of the maximum-thickness point which for these tests was at the 50-percent-chord point. It is predicted in reference 2 that an increase in pressure drag at the lower supersonic Mach numbers accompanies a rearward shift of the maximum thickness from 20 to 50 percent of the chord, but possible effects on the other aerodynamic characteristics are not indicated by the existing linear theories.

## SYMBOLS

- b span of wing, feet
- c local wing chord, feet
- $\bar{c}$  mean aerodynamic chord  $\left( \frac{\int_0^{b/2} c^2 dy}{\int_0^{b/2} c dy} \right)$ , feet
- $C_D$  drag coefficient  $\left( \frac{\text{drag}}{qS} \right)$
- $C_{D_{\min}}$  minimum drag coefficient
- $\Delta C_D$  change in drag coefficient from value of minimum drag coefficient ( $C_D - C_{D_{\min}}$ )
- $\frac{\Delta C_D}{\Delta C_L^2}$  drag-rise factor
- $C_L$  lift coefficient  $\left( \frac{\text{lift}}{qS} \right)$

$\Delta C_L$	change in lift coefficient from the value at minimum drag coefficient ( $C_L - C_{L_{D=\min}}$ )
$\frac{dC_L}{d\alpha}$	lift-curve slope at zero lift coefficient, per degree
$C_m$	pitching-moment coefficient $\left( \frac{\text{moment about centroid of area of wing}}{qSC} \right)$
$\frac{L}{D}$	lift-drag ratio $\left( \frac{\text{lift}}{\text{drag}} \right)$
$\left( \frac{L}{D} \right)_{\max}$	maximum lift-drag ratio
M	free-stream Mach number
q	free-stream dynamic pressure $\left( \frac{1}{2} \rho V^2 \right)$ , pounds per square foot
R	free-stream Reynolds number referred to the mean aerodynamic chord
S	wing area, square feet
V	free-stream velocity, feet per second
y	spanwise distance from the wing root-chord line, feet
$\alpha$	angle of attack, degrees
$\rho$	free-stream mass density, slugs per cubic foot

#### APPARATUS AND TESTS

The experimental investigation was carried out in the Ames 1- by 3-1/2-foot high-speed wind tunnel, a single-return closed-throat type vented to atmospheric air. The tunnel was equipped with a flexible-throat assembly (fig. 1) to permit a variation in Mach number above unity.

The model (fig. 2) was constructed of steel according to the dimensions of figure 3. The radii of the leading and trailing edges of the wing were less than 0.002 inch, and the wing surfaces were ground but not polished.

The wing was mounted in a horizontal plane in a slender body of revolution (fig. 2) having the minimum size consistent with its function as an adequate support. A series of identical bodies (fig. 3), sting supported at different angles of attack, was employed interchangeably to vary the wing angle of attack.

A three-component electrical strain-gage balance was used to measure the lift, drag, and pitching moment of the model. Measurements of the pressure acting on the base of the body were made simultaneously with the force measurements.

The aerodynamic characteristics of the model were determined at angles of attack between  $-3^\circ$  and  $9^\circ$  over a range of Mach numbers from 0.50 to 1.49. Between Mach numbers of 0.975 and 1.09 choked-flow conditions prevailed in the tunnel test section, precluding the determination of the aerodynamic characteristics within this range. Reynolds numbers, based on the mean aerodynamic chord of the model, varied from approximately  $0.67 \times 10^6$  at a Mach number of 0.50 to  $0.83 \times 10^6$  at 1.49.

#### REDUCTION OF DATA

The wing area used in computing the force and moment coefficients includes the portion enclosed within the body. The pitching-moment coefficients are based upon the mean aerodynamic chord and were referred to the centroid of area of the wing.

Allowance was made for several interference effects peculiar to the wind tunnel. The drag and angle-of-attack measurements in the subsonic Mach number range have been corrected for tunnel-wall interference by the method outlined in reference 5. These corrections, shown in reference 6 to be independent of Mach number, were

$$\Delta\alpha = 0.424 C_L$$

$$\Delta C_D = 0.0075 C_L^2$$

All of the drag data have been corrected for buoyant pressure gradients existing in the test section of the wind tunnel. This correction was less than 2 percent of the minimum drag at all Mach numbers. No corrections to the measured characteristics have been attempted for the effects of air-stream inclination. The corrections for the effects of tunnel blockage were of negligible magnitude.

Further correction of the drag data was required as a result of an interfering pressure field at the base of the support body arising from the proximity of the end of the balance housing to the body. On the basis of reference 7 the effect of this pressure field is believed to be confined to the base of the body at all supersonic Mach numbers.

At subsonic Mach numbers it was concluded from theoretical considerations that aside from changes in the base pressure this interference did not extend sufficiently far beyond the base to influence the results. The effects of the interference at each Mach number were compensated by subtracting from the measured drag the force resulting from the difference between the free-stream static pressure and the test pressure exerted on the base area. Although this correction is not exact, since the true pressure differences at the base were not known, all drag forces are referred to a common basis for comparison.

## RESULTS AND DISCUSSION

The results of the tests are presented in figure 4 which shows, for each test Mach number, lift coefficient as a function of angle of attack, and pitching-moment coefficient, drag coefficient, and lift-drag ratio as functions of lift coefficient. The variations with Mach number of these characteristics are shown in figures 5 to 11, inclusive. Schlieren photographs of the flow field about the model and support, taken during force measurements, are presented in figure 12. Defects of the optical system are shown in figure 12(a). The defects appear in all the schlieren photographs and should not be confused with the flow field. To show the effect on the aerodynamic characteristics of a change in the location of maximum thickness of the wing, the results of reference 4 for the 20-percent-chord location of maximum thickness are also included in several figures. The calculated characteristics shown were determined by the methods given in references 1, 2, and 3, and pertain to the wing alone. Experimental results from reference 7 for an identical wing and body at a Mach number of 1.53 and a Reynolds number of  $1 \times 10^8$ , and similar results from unpublished data on file at the Ames Aeronautical Laboratory for a wing alone at a Mach number of 0.13 and a Reynolds number of  $15.4 \times 10^6$  are also included. In comparing the latter results with those of the present investigation, consideration should be given to the large differences in Reynolds number and in the method of model support (three-strut support in the latter case).

The interference occurring between the wing and the support body could not be readily evaluated; consequently, the force coefficients are presented for the wing and body in combination rather than for the wing alone. It is indicated in reference 7 for a Mach number of 1.53 that the contribution of the body to the total lift and pitching moment is small, and on this basis it is believed that the results presented here for the combination may be considered sensibly representative of the wing at all Mach numbers. In view of the applied

base-drag correction described previously, however, the drag coefficients are not strictly representative of either the combination or the wing alone.

### Lift Characteristics


With reference to figure 4, it is observed that the curve of the lift coefficient against angle of attack is not linear, the slope being greater at the higher angles of attack. Although this condition is not predicted by the first-order theories of references 1 and 2, it is generally characteristic of wings of very low aspect ratio.

In figure 5, the steady increase of lift-curve slope at zero angle of attack with Mach number below 0.975 is seen to be in accord with the trends of the calculated values for subsonic Mach numbers (reference 1) for a lifting vortex line. At supersonic Mach numbers the gradual decrease of the lift-curve slope above a Mach number of 1.12 conforms with the trend of the calculated slopes for a flat lifting plate (reference 2). It is evident that at supersonic Mach numbers, slightly lower values of lift-curve slope result from a change in the position of maximum thickness from 20 to 50 percent of the chord; whereas at subsonic Mach numbers the respective magnitudes are nearly equal. This difference in the values of lift-curve slope at supersonic Mach numbers is not accounted for by the theory of reference 2, which ignores the effect of profile shape, and thus can probably be attributed to a second-order effect of thickness distribution. The results from reference 5 and the unpublished data for a Reynolds number of  $15.4 \times 10^6$ , also plotted in the figures, are in fair agreement with the results of the present investigation.

In figure 6, it is to be noted that the sharp irregularities and sudden losses in lift that are characteristic of unswept wings of higher aspect ratio at transonic Mach numbers are absent for the wing investigated. With regard to the region between Mach numbers 0.975 and 1.09 in figures 5 and 6, it is expected, on the basis of wing-flow tests of similar configurations in this range, that curves of subsonic and supersonic characteristics could be faired smoothly.

### Drag Characteristics

The drag characteristics of the wing under investigation can best be discussed by treating separately the respective variations of drag coefficient with lift coefficient and Mach number.



The effect of lift coefficient on the drag coefficient is shown by the polars of figure 4, where for supersonic Mach numbers, the calculated values are also plotted for comparison with the experimental results. In the calculations the drag resulting from skin friction of the wing alone was determined through the application of the results of reference 8. Because attempts to determine the actual distribution of laminar and turbulent boundary-layer flow on the model wing by means of the liquid-film technique discussed in reference 7 were unsuccessful, the calculations were made for completely laminar and for completely turbulent flow, those being the respective minimum and maximum values of skin-friction drag for the wing. The remaining portion of the drag was calculated by the methods of reference 2 under the assumption that there was no leading-edge suction. The principal conclusion to be drawn from inspection of the polars in figure 4 is the fact that, with the exception of the curves for Mach numbers 1.09 and 1.12, the experimental polars are generally in fair agreement with those from theory. When notation is made of the discrepancies between the test results and the theoretical characteristics at these two Mach numbers, it is evident that in the region of high lift coefficients the drag coefficients are lower than would be expected from examination of the drag polars for the other Mach numbers. Possible explanations for the discrepancies are offered in the discussion of the variation of drag coefficient with Mach number to follow.

The results of the investigation pertaining to drag coefficient as a function of Mach number are summarized in figure 7. Inspection of this figure reveals two noteworthy features in the curves for the higher lift coefficients: (1) The slopes of the curves are negative for subsonic and positive for supersonic Mach numbers (due to the variation of the drag due to lift, as will be shown later), and (2) the values of drag coefficient in the region of Mach numbers from 1.09 to approximately 1.17 appear unexpectedly low in relation to the rest of the curve. Although a great deal of effort was expended to ascertain the cause of these low drag coefficients, no adequate explanation was found. It was concluded, however, that for the following reasons these low values are probably a result of wind-tunnel-interference effects rather than genuine values which could be expected in free air:

1. The tunnel air stream at low supersonic Mach numbers is known to contain extraneous and random shock waves, examples of which are indicated by arrows in figures 12(d) and (e).

2. The reflections from the tunnel walls of the shock waves originating at the nose of the model body, and at the juncture of the leading edge of the wing with the body, impinged on the model at Mach



numbers from 1.09 to 1.17. The effect of these reflected waves on the drag data could not be readily assessed, but it is believed to have caused a reduction in the drag forces.

3. As is evident in the schlieren photographs of figure 12, at the lowest supersonic test Mach number, a strong normal shock wave stood immediately aft of the wing trailing edge and its effect could have been communicated to the wing through the wing wake as a buoyant force in a direction tending to reduce the drag.

To further the analysis of the test results and to facilitate comparison of those results with the characteristics predicted by theoretical methods, the drag of the model has been separated into two parts, the drag due to lift and the minimum drag of the model. The parameter used to indicate the amount of drag due to lift, valid because the experimental polars are parabolic, is the drag-rise factor, which is defined as follows:

$$\frac{\Delta C_D}{\Delta C_L^2} = \frac{C_D - C_{D_{min}}}{\Delta C_L^2}$$

The drag-rise factor is presented in figure 8, where a comparison is made with the reciprocal of the experimental lift-curve slope for the wing under investigation.

It can be shown algebraically that the drag-rise factor of a flat plate realizing no leading-edge suction<sup>1</sup> and inclined to the air stream at small angles of attack is equal to the reciprocal of the lift-curve slope. The general agreement between the values thus calculated and the observed values indicates that the drag characteristics of this wing closely resemble those of the corresponding flat plate and that very little leading-edge suction is obtained. With reference again to figure 7, it is concluded that the respective negative and positive slopes at subsonic and supersonic Mach numbers of the curves of drag coefficient as a function of Mach number at the higher lift coefficients are due to the variation in the drag-rise factor with Mach number.

The effect of Mach number upon the minimum drag coefficient, shown in figure 9, is negligible in the subsonic range, a result which is supported by the calculated variation with Mach number of the drag coefficient associated with skin friction. The actual

---

<sup>1</sup>Discussed in Aerodynamic Theory, vol. IV, pp. 27-29, Durand, and in reference 5.

---

distribution of laminar and turbulent flow in the boundary layer not being known for the test model, curves representing the maximum and minimum skin friction are shown in the figure. Between Mach numbers of 0.95 and 1.2 a continuous rise in the minimum drag of the wing is noted. The experimental results for virtually the entire range of supersonic Mach numbers fall within the respective limits of the drag coefficient which have been calculated as the sum of the pressure drag and the skin-friction drag for the laminar and the turbulent boundary-layer flow. The discontinuities in these calculated limits at a Mach number of 1.41 correspond to a coincidence of the Mach cone emanating from the apex of the ridge line of the wing and the ridge line itself. The test points were not spaced closely enough to determine experimentally the existence of such a discontinuity.

The minimum drag coefficients observed between Mach numbers of 1.09 and 1.3 are lower for the wing having the maximum thickness at 20 percent of the chord than those for the wing of the present investigation, these relative magnitudes being in accord with the predictions of reference 2 with regard to the effect of maximum-thickness location. The reversal in the relative magnitudes of the drag coefficients for the two wings above 1.3 Mach number can probably be attributed to changes in the drag resulting from skin friction, since the theoretical pressure drags for the two wings do not vary sufficiently within the experimental range of supersonic Mach numbers to account for the observed differences. With increasing Mach number above 1.41, it is possible that increasingly greater surface areas become exposed to falling pressure gradients for the wing with maximum thickness at midchord, such that greater areas of laminar boundary-layer flow and therefore lesser skin friction result for this wing. Evidence supporting this conclusion is to be found in reference 7 for a Mach number of 1.53.

If consideration again be given to the differences in the Reynolds numbers of the respective tests, the minimum drag coefficients taken from reference 7 and from unpublished data on file at the Ames Aeronautical Laboratory for a Reynolds number of  $15.4 \times 10^6$  are in satisfactory agreement with the results of the present investigation shown in figure 9.

Figure 10 summarizes the results of the investigation pertaining to maximum lift-drag ratio. Values of the maximum lift-drag ratio obtained from other sources (noted on the figure) are in fair agreement if differences in the method of support are taken into account. The apparently high lift-drag ratios at the lower supersonic Mach numbers can most probably be attributed to the unexpectedly low drag

values observed in the region of Mach numbers from 1.09 to approximately 1.2.

The values of maximum lift-drag ratio at supersonic Mach numbers for the wing with maximum thickness at 20 percent of the chord are somewhat greater than those for the wing of the present investigation by virtue of the more favorable drag characteristics of the former (cf. fig. 7).

#### Pitching-Moment Characteristics

The curves of pitching-moment coefficient as a function of lift coefficient in figure 4 were used to determine the location at zero lift coefficient of the aerodynamic center in percent of the mean aerodynamic chord. The variation with Mach number of the position of the aerodynamic center is shown in figure 11. It is noted from this figure that the aerodynamic center shifts rearward from 42 percent of the mean aerodynamic chord toward the centroid of area of the wing (located at 50 percent of the mean aerodynamic chord) as the Mach number of unity is approached, and that above 1.09 it coincides with the centroid. It is predicted in reference 2 that the centroid and the aerodynamic center of a flat triangular plate will coincide at supersonic Mach numbers. The fact that the location of maximum thickness of the wing does not significantly affect the pitching-moment characteristics at supersonic Mach numbers is also indicated in figure 11. At subsonic Mach numbers a more rearward position of the aerodynamic center is indicated when the maximum-thickness location is changed from 20 to 50 percent of the chord.

#### CONCLUSIONS

The results of wind-tunnel tests of a thin triangular wing of aspect ratio 2 and symmetrical double-wedge profile with maximum thickness at midchord in the Mach number ranges from 0.50 to 0.975 and 1.09 to 1.49, and comparison of these results with those for a similar wing with maximum thickness at 20 percent of the chord indicated the following:

1. The lift coefficient at a constant angle of attack for either maximum-thickness location varied continuously and regularly with Mach number below 0.975 and above 1.09.

2. The lift-curve slope increased with Mach number below 0.97 and decreased at Mach numbers greater than 1.13. A decrease in the lift-curve slope at supersonic Mach numbers accompanied a change in

the location of maximum thickness from 20 to 50 percent of the chord.

3. The drag coefficient at a constant lift coefficient decreased continuously with increasing Mach number below 0.9 and increased continuously above 1.09 at lift coefficients greater than 0.1. Somewhat higher drag coefficients for the most part resulted for the profile with maximum thickness at 50 rather than 20 percent of the chord.

4. A rise with Mach number in the minimum drag coefficient occurred between Mach numbers of 0.95 and 1.2. At Mach numbers greater than 1.2 the minimum drag of the wing with maximum thickness at midchord decreased, becoming less than that of the wing with maximum thickness at 20 percent of the chord at Mach numbers greater than 1.3.

5. The maximum lift-drag ratios remained virtually constant in both the subsonic and supersonic Mach number ranges, and were approximately 25 percent lower at supersonic Mach numbers. The maximum lift-drag ratios were slightly lower at supersonic Mach numbers for the wing with the maximum thickness located at 50 rather than 20 percent of the chord.

6. The aerodynamic center of the wing with maximum thickness at 50 percent of the chord in the subsonic Mach number range moved aft from 42 to 51 percent of the mean aerodynamic chord. Throughout the supersonic range it coincided with the centroid of area of the wing. Similar changes in position of the aerodynamic center were observed for the wing with the maximum thickness at 20 percent of the chord.

Ames Aeronautical Laboratory,  
National Advisory Committee for Aeronautics,  
Moffett Field, Calif.

#### REFERENCES

1. DeYoung, John: Theoretical Additional Span Loading Characteristics of Wings with Arbitrary Sweep, Aspect Ratio, and Taper Ratio. NACA TN No. 1491, 1947.
2. Puckett, A. E., and Stewart, H. J.: Aerodynamic Performance of Delta Wings at Supersonic Speeds. Jour. Aero. Sci., vol. 14, no. 10, Oct. 1947, pp. 567-578.

3. Jones, Robert T.: Estimated Lift-Drag Ratios at Supersonic Speed. NACA TN No. 1350, 1947.
4. Berggren, Robert E., and Summers, James L.: Aerodynamic Characteristics at Subsonic and Supersonic Mach Numbers of a Thin Triangular Wing of Aspect Ratio 2. I - Maximum Thickness at 20 percent of the Chord. NACA RM No. A8116, 1948.
5. Glauert, H.: Wind Tunnel Interference on Wings, Bodies, and Airscrews. R. & M. No. 1566, British, A. R. C., 1933.
6. Goldstein, S., and Young, A.D.: The Linear Perturbation Theory of Compressible Flow with Applications to Wind-Tunnel Interference. R. & M. No. 1909, British, A. R. C., 1943.
7. Vincenti, Walter G., Nielsen, Jack N., and Matteson, Frederick H.: Investigation of Wing Characteristics at a Mach Number of 1.53. I - Triangular Wings of Aspect Ratio 2. NACA RM No. A7110, 1947.
8. Theodorsen, Theodore, and Regier, Arthur: Experiments on Drag of Revolving Disks, Cylinders, and Streamline Rods at High Speeds. NACA TR No. 793, 1944.

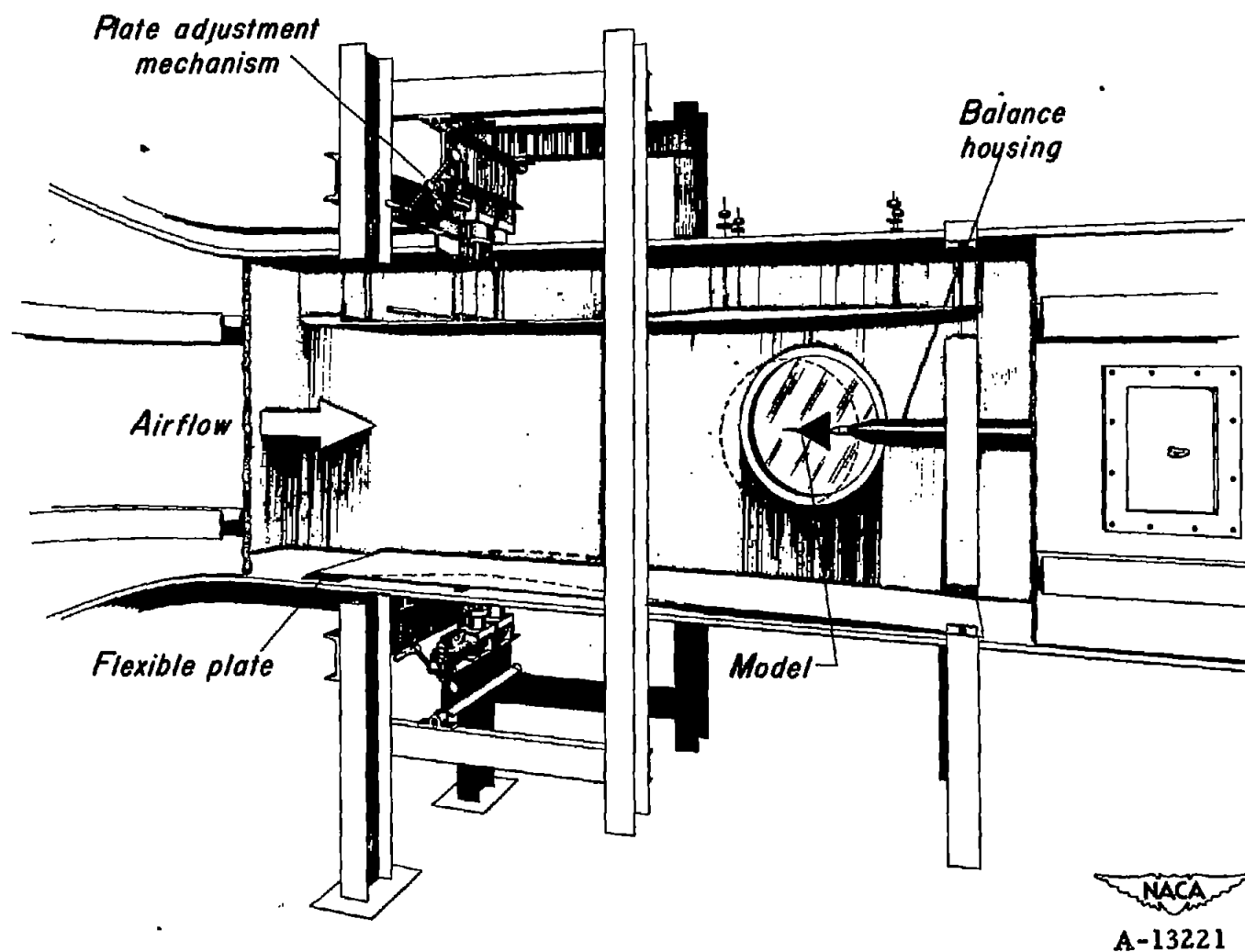
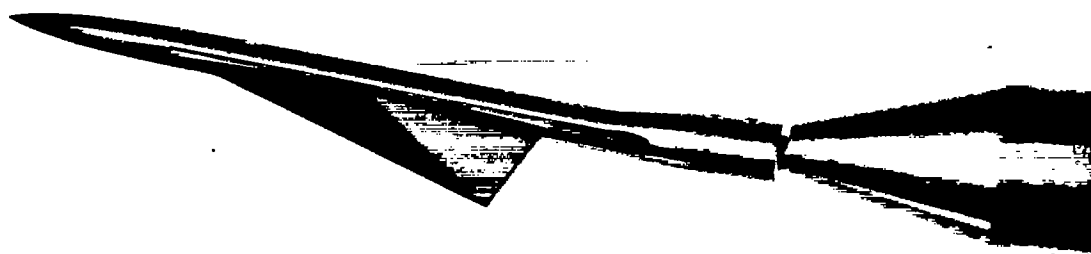


Figure 1.- Illustration of the flexible-throat mechanism in the Ames  
1-by 3-1/2-foot high-speed wind tunnel.





NACA  
A-12050

Figure 2.— Photograph of triangular wing and body.





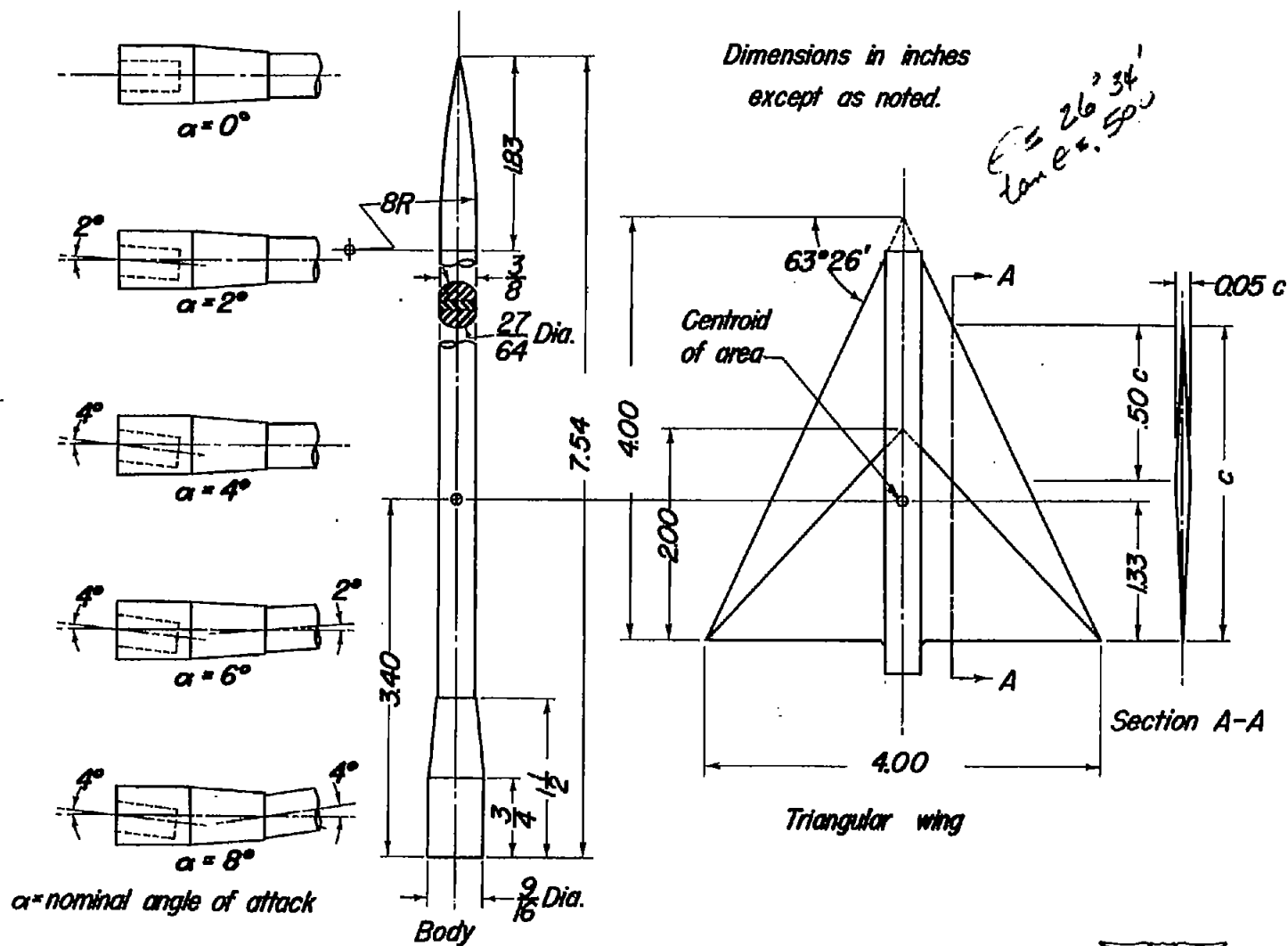


Figure 3.- Sketch of triangular wing and body.

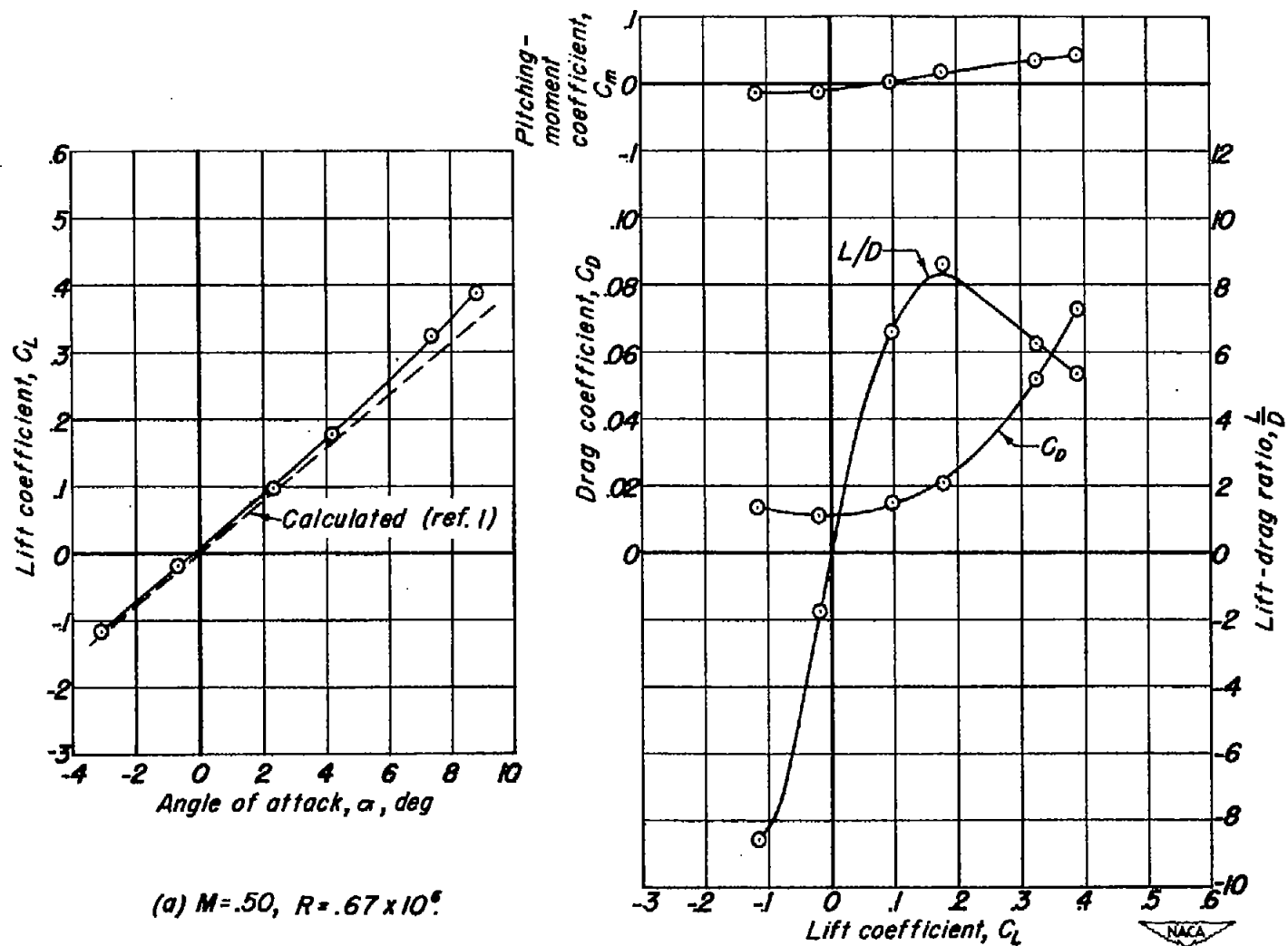


Figure 4.— The aerodynamic characteristics of the triangular wing and supporting body at Mach numbers ranging from 0.50 to 1.49.

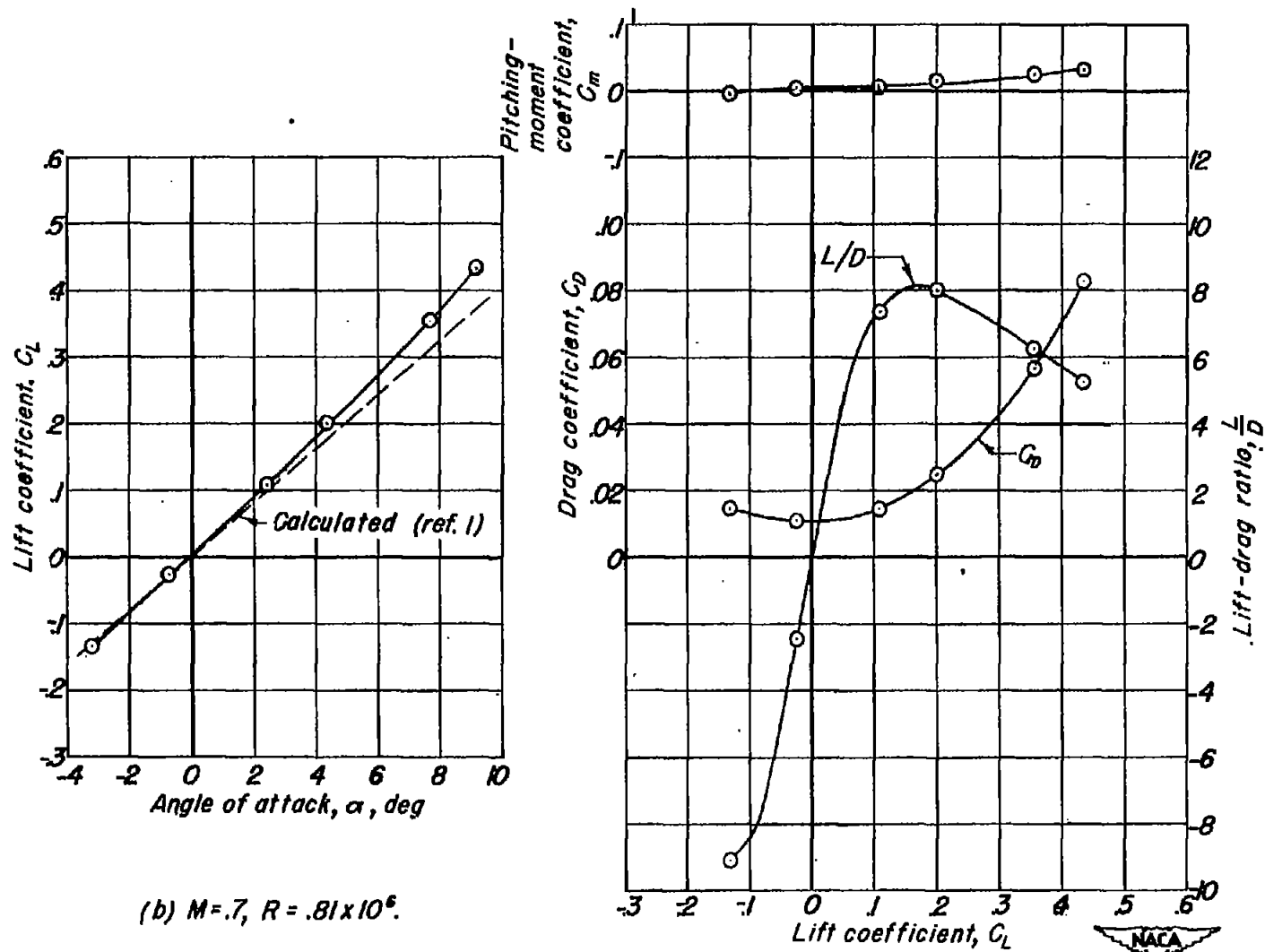
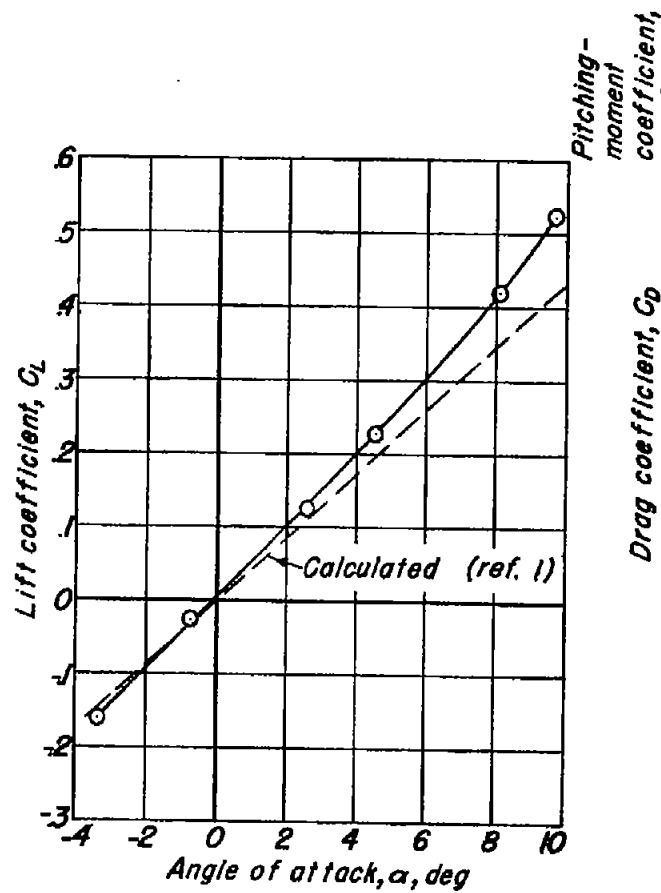
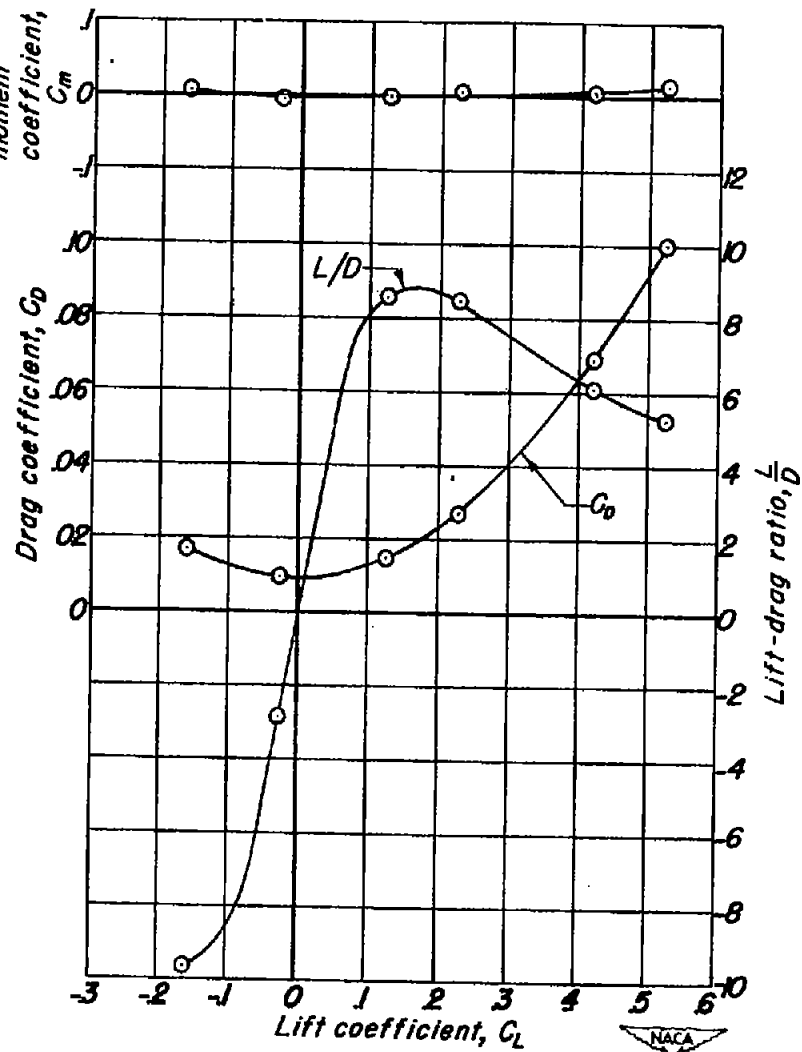


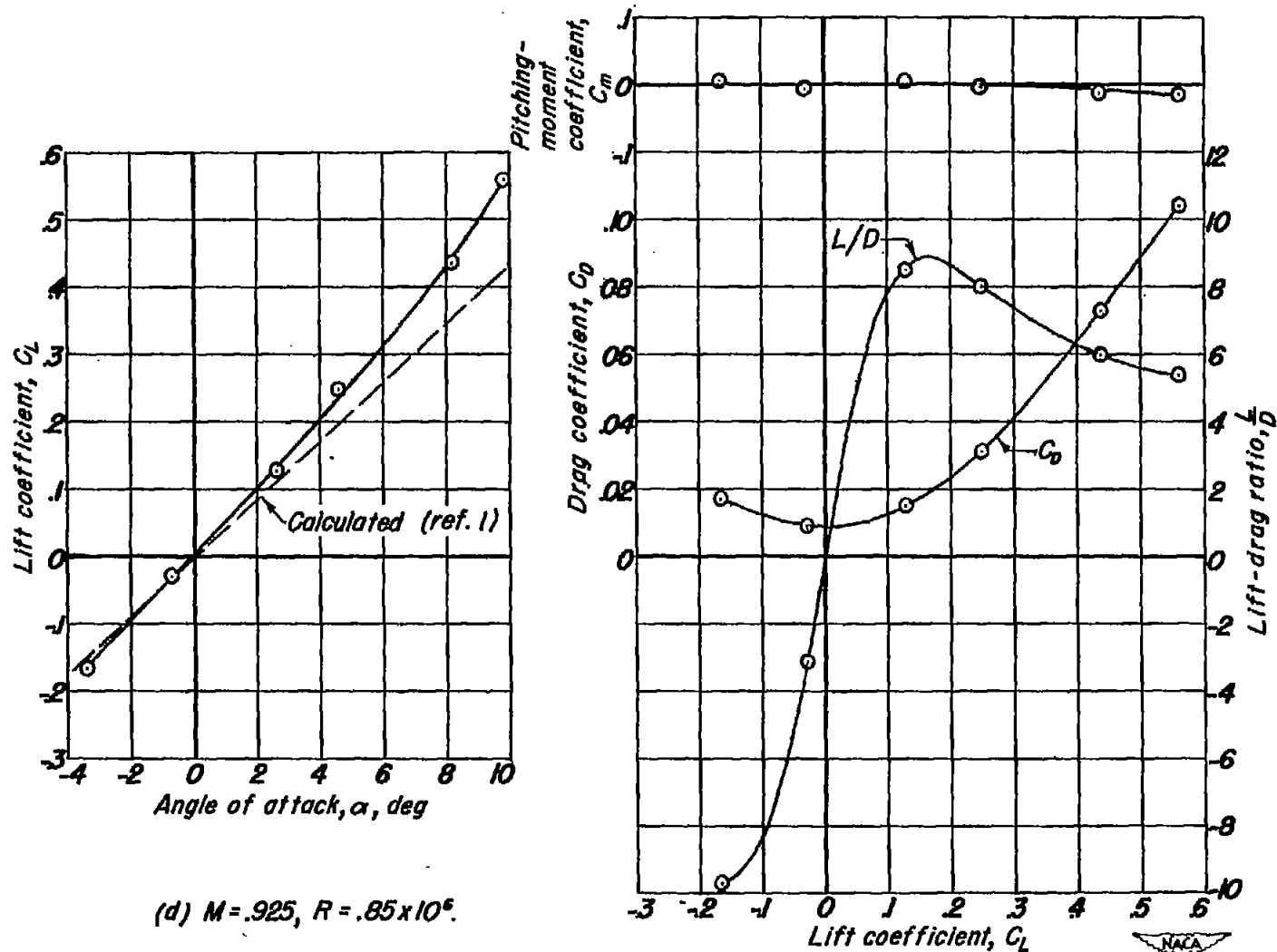
Figure 4.- Continued.



(c)  $M = .9$ ,  $R = .85 \times 10^6$

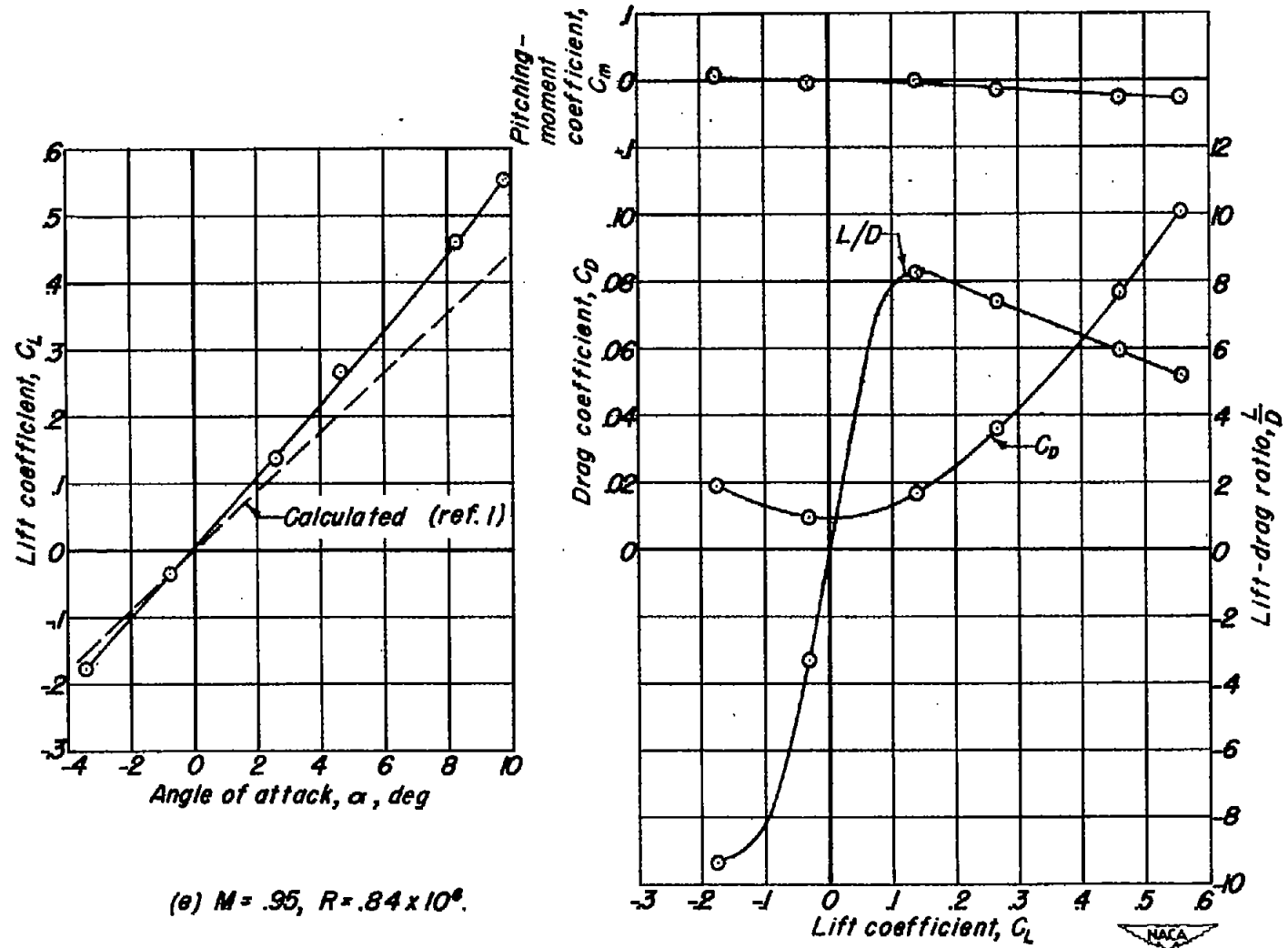
Figure 4 - Continued.





(d)  $M = .925$ ,  $R = .85 \times 10^6$ .

Figure 4. - Continued.



(a)  $M = .95$ ,  $R = .84 \times 10^6$ .

Figure 4. - Continued.

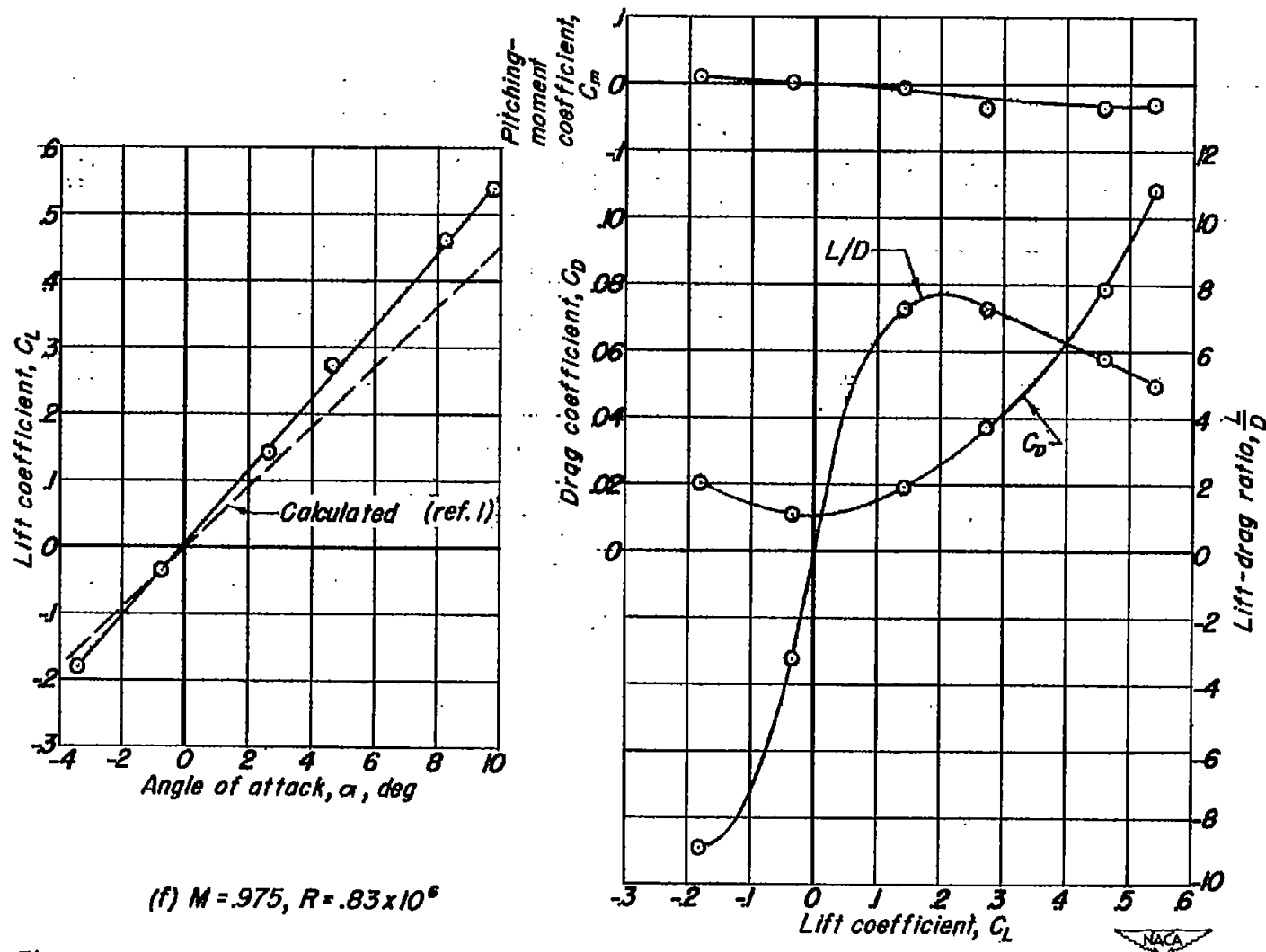


Figure 4. - Continued.



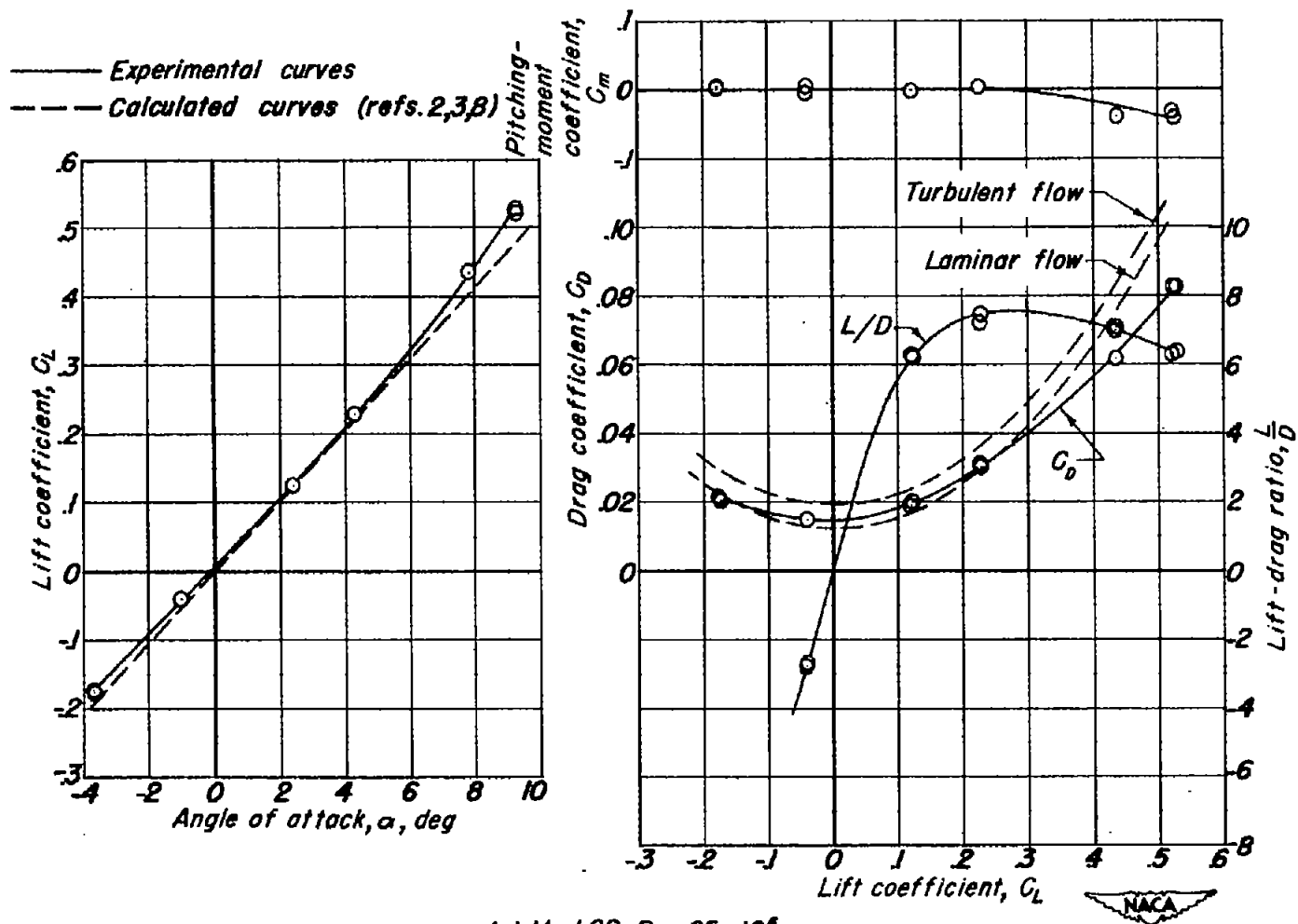


Figure 4. - Continued.

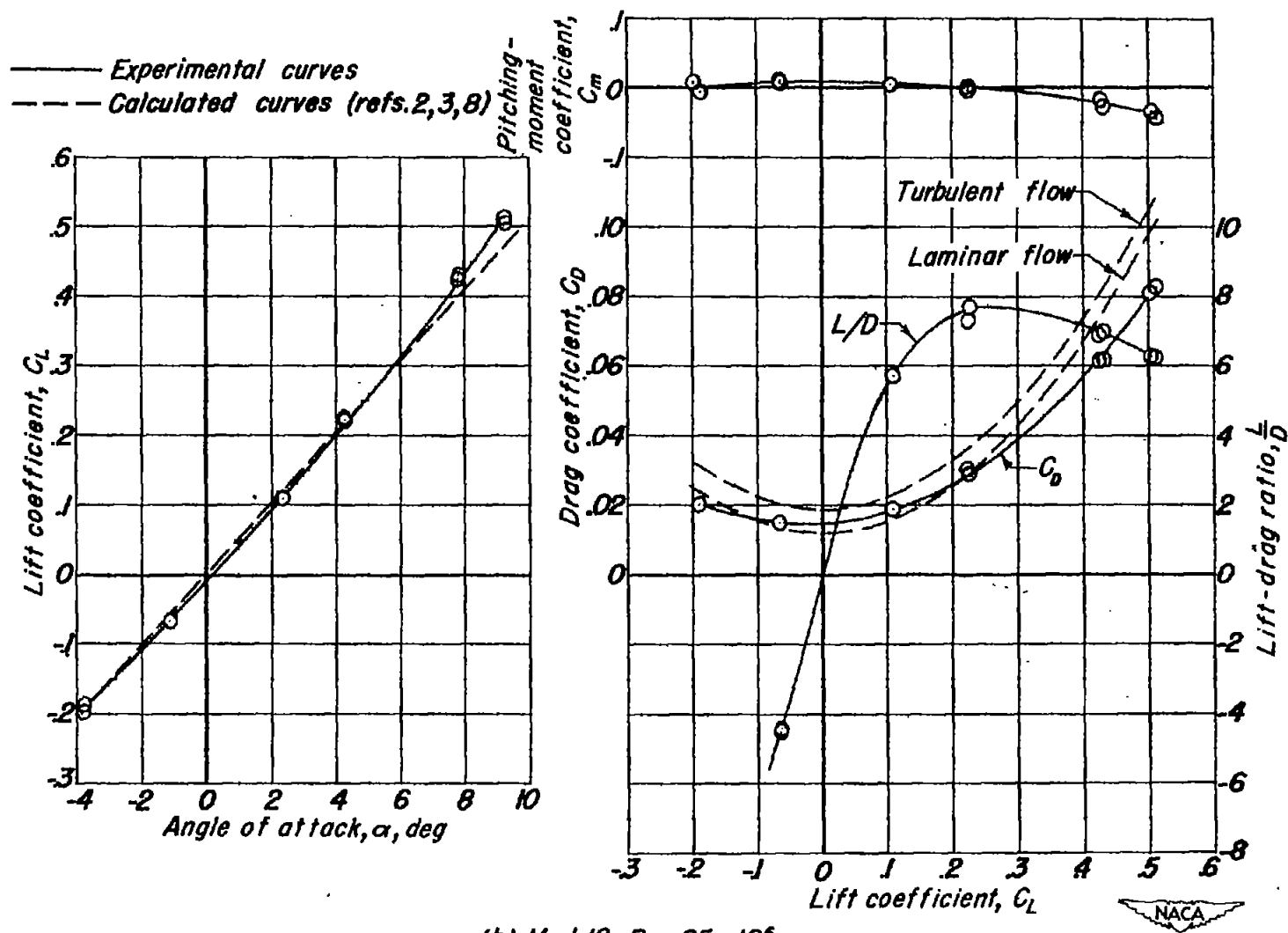
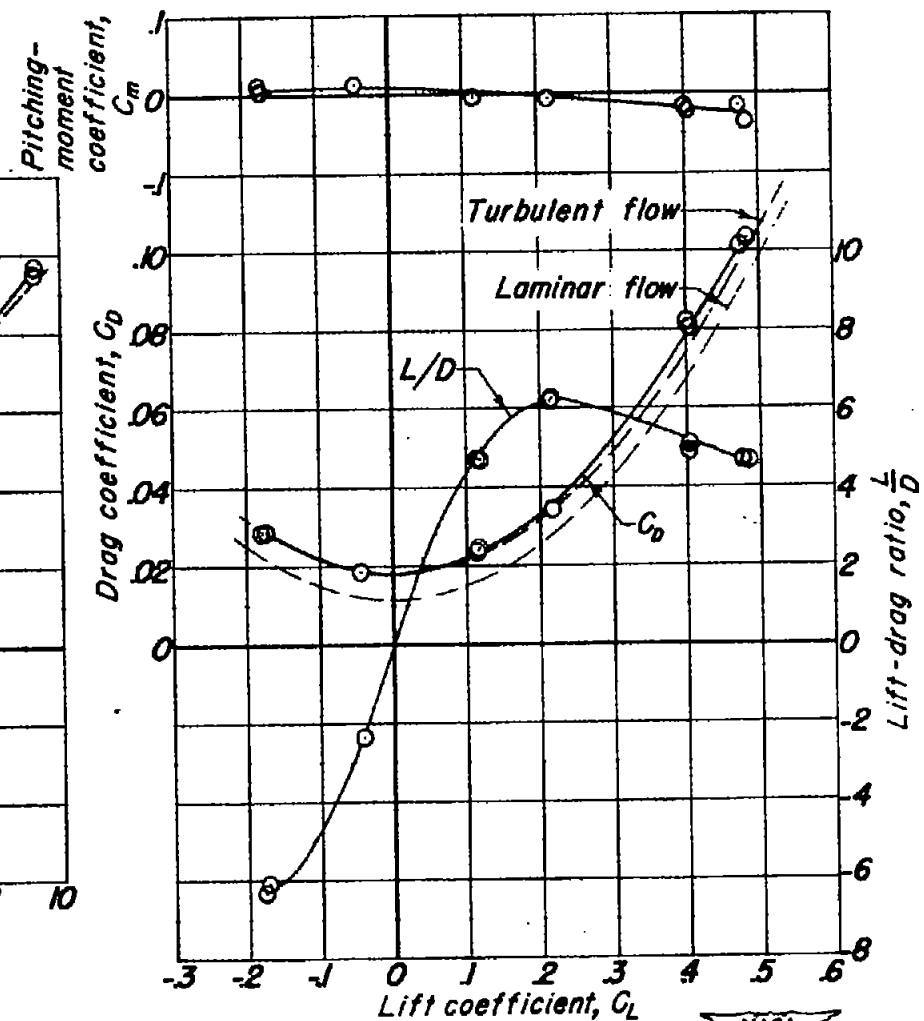
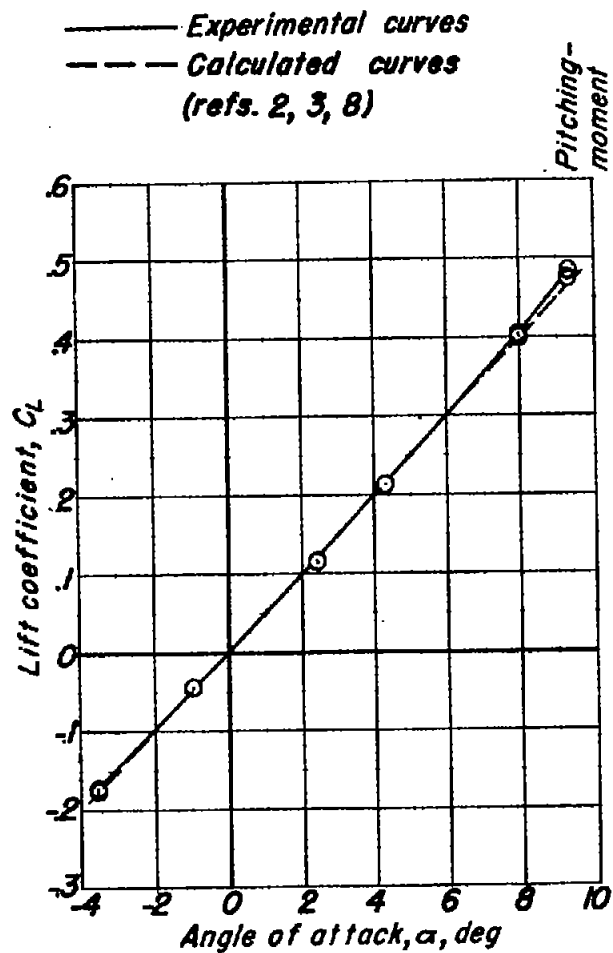
(h)  $M = 1.12$ ,  $R = .85 \times 10^6$ .

Figure 4.—Continued.



(1)  $M=1.17$ ,  $R = .85 \times 10^6$ .

Figure 4.—Continued.

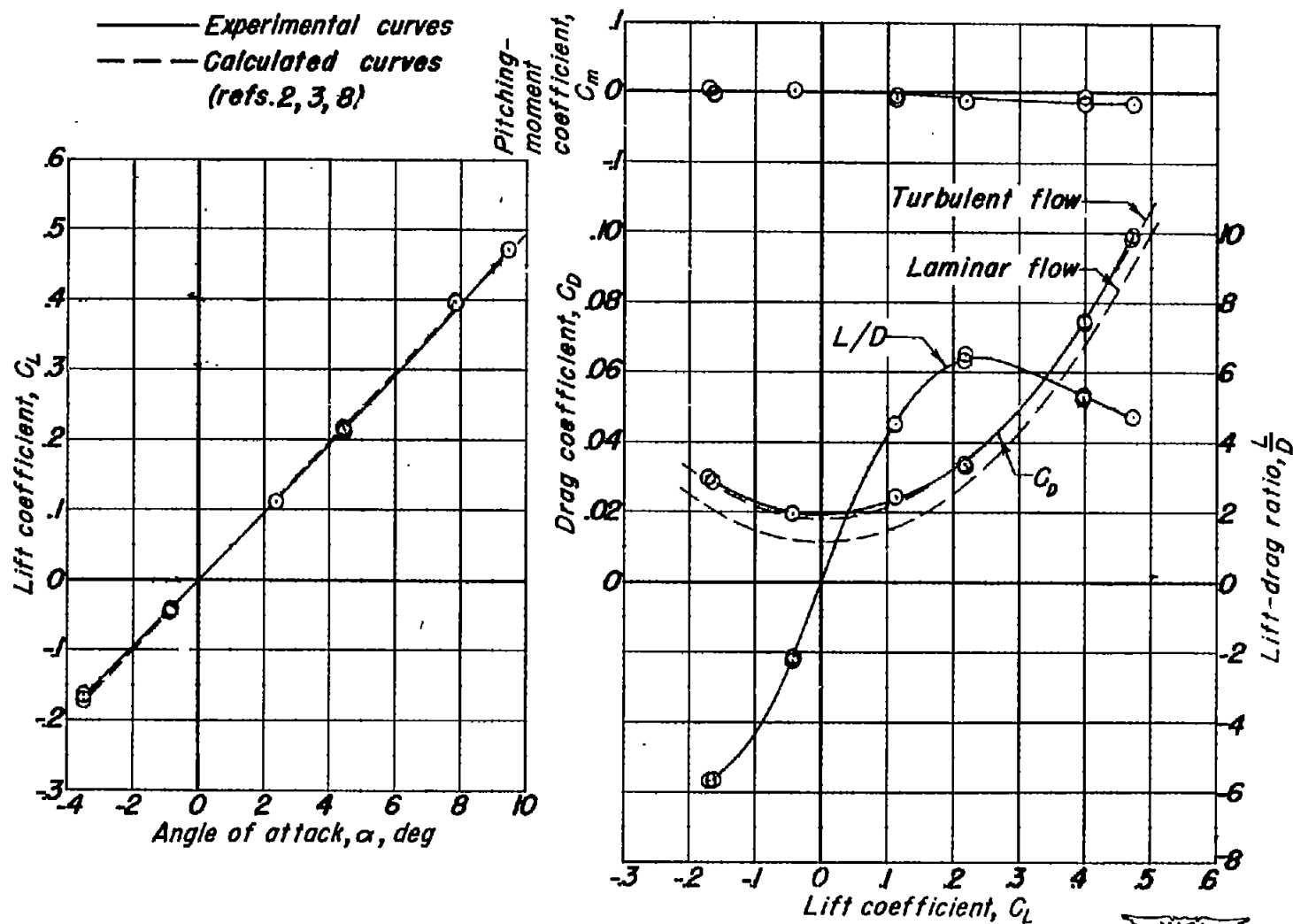
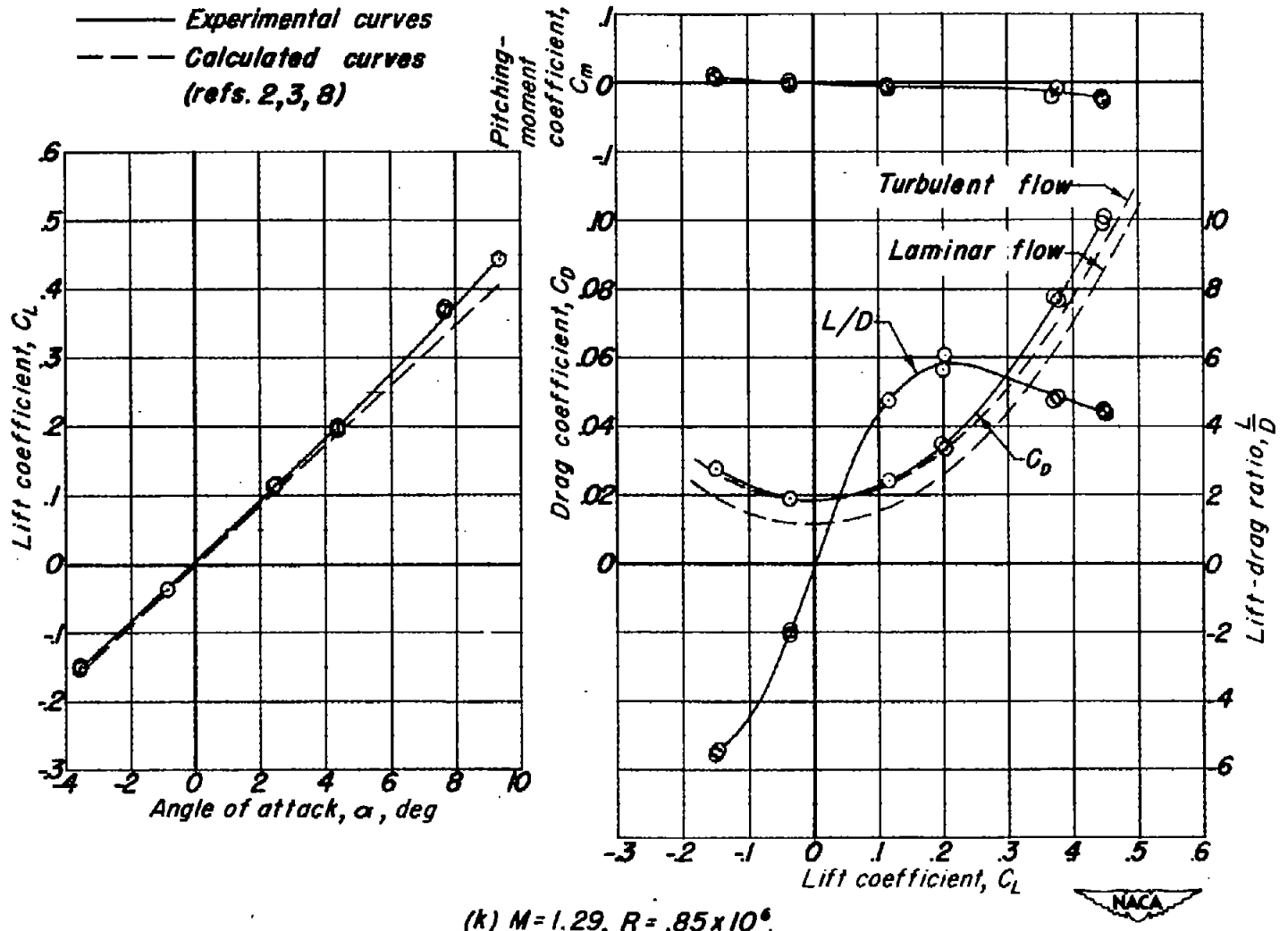
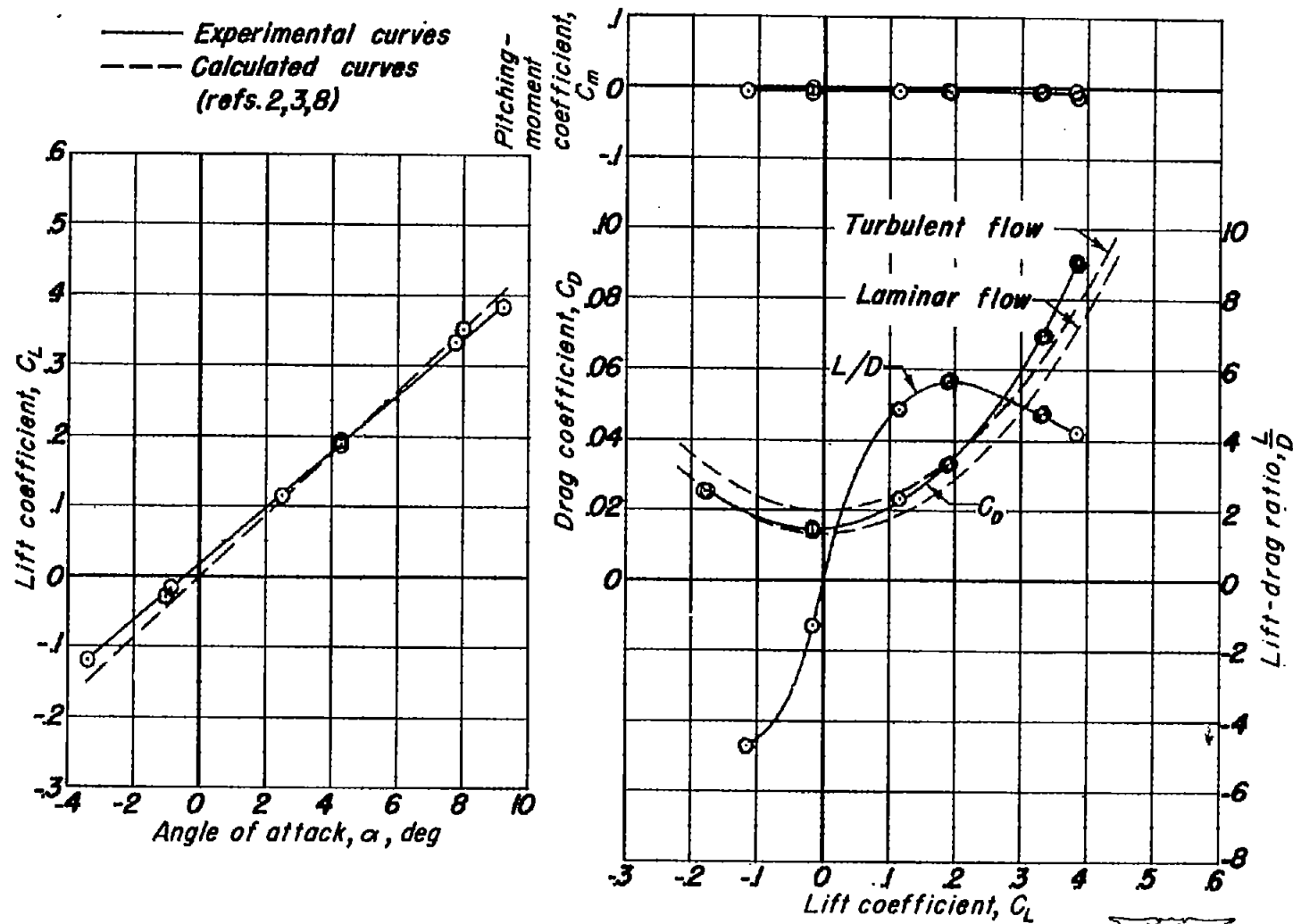
(j)  $M=1.20$ ,  $R=.85 \times 10^6$ .

Figure 4. - Continued.



(k)  $M=1.29$ ,  $R=.85 \times 10^6$

Figure 4.—Continued.



(1)  $M=1.49$ ,  $R=.83 \times 10^6$

Figure 4. - Concluded.

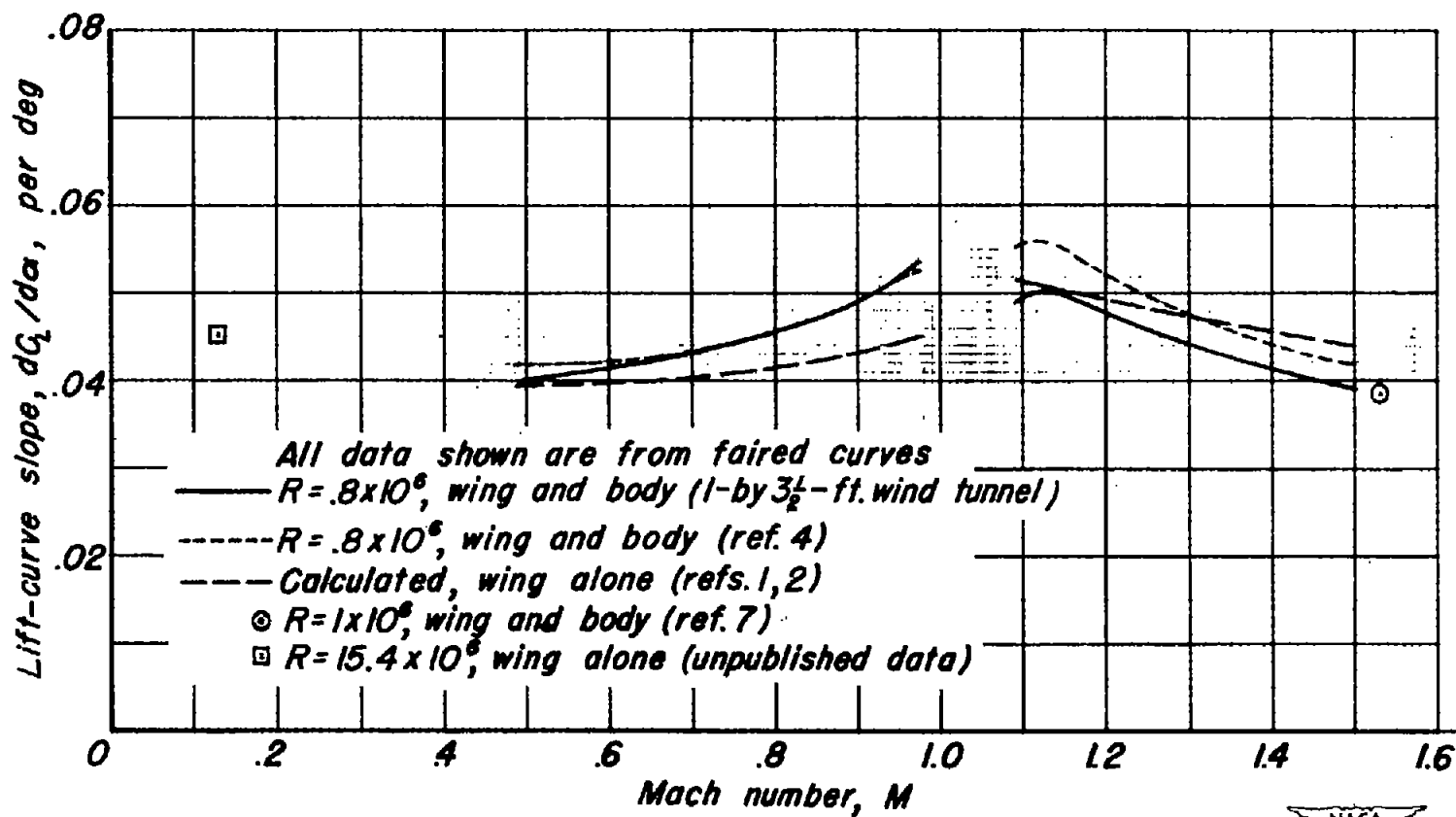


Figure 5.— The variation of lift-curve slope at zero lift with Mach number.

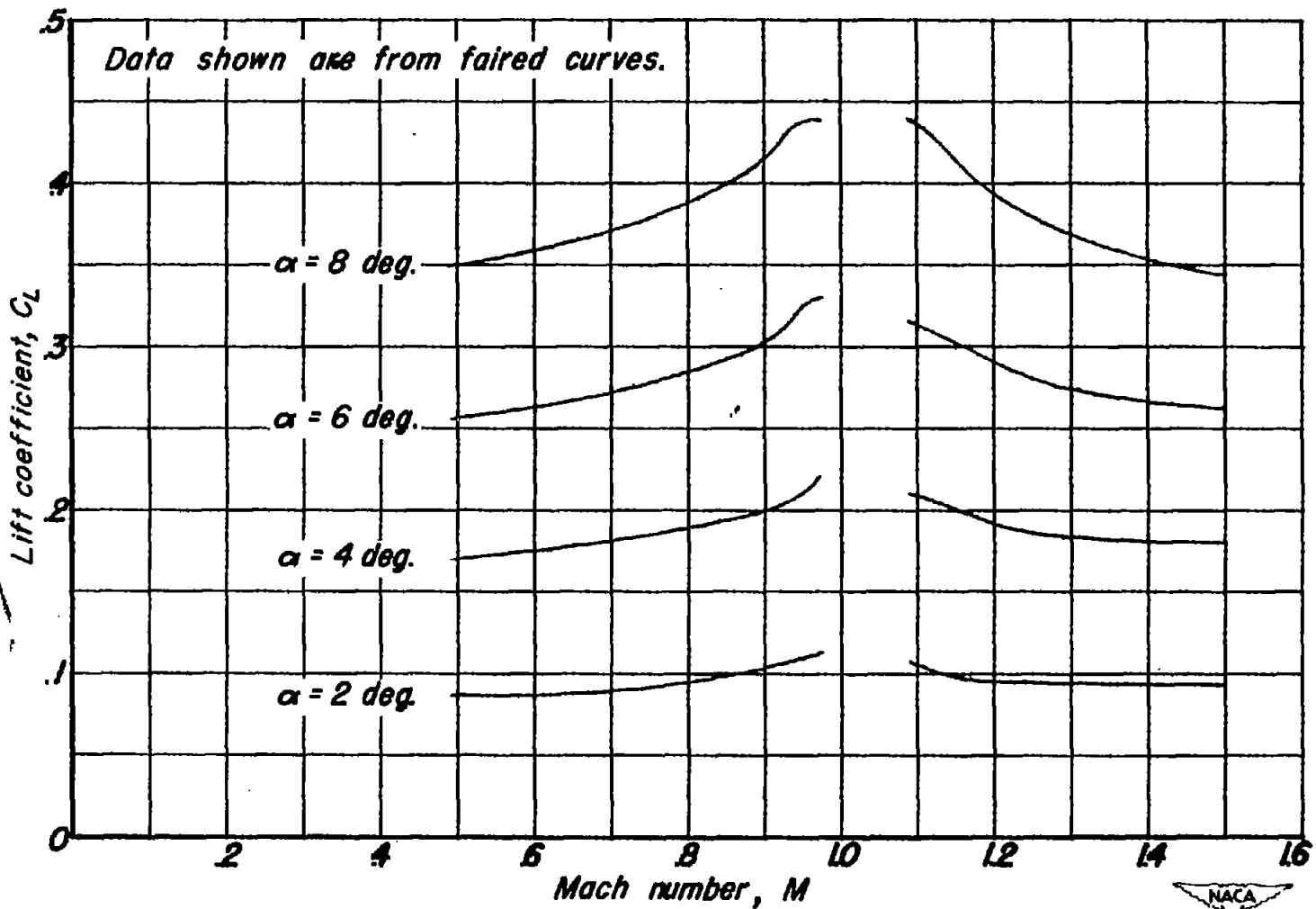


Figure 6.— The variation of lift coefficient with Mach number at constant angle of attack.



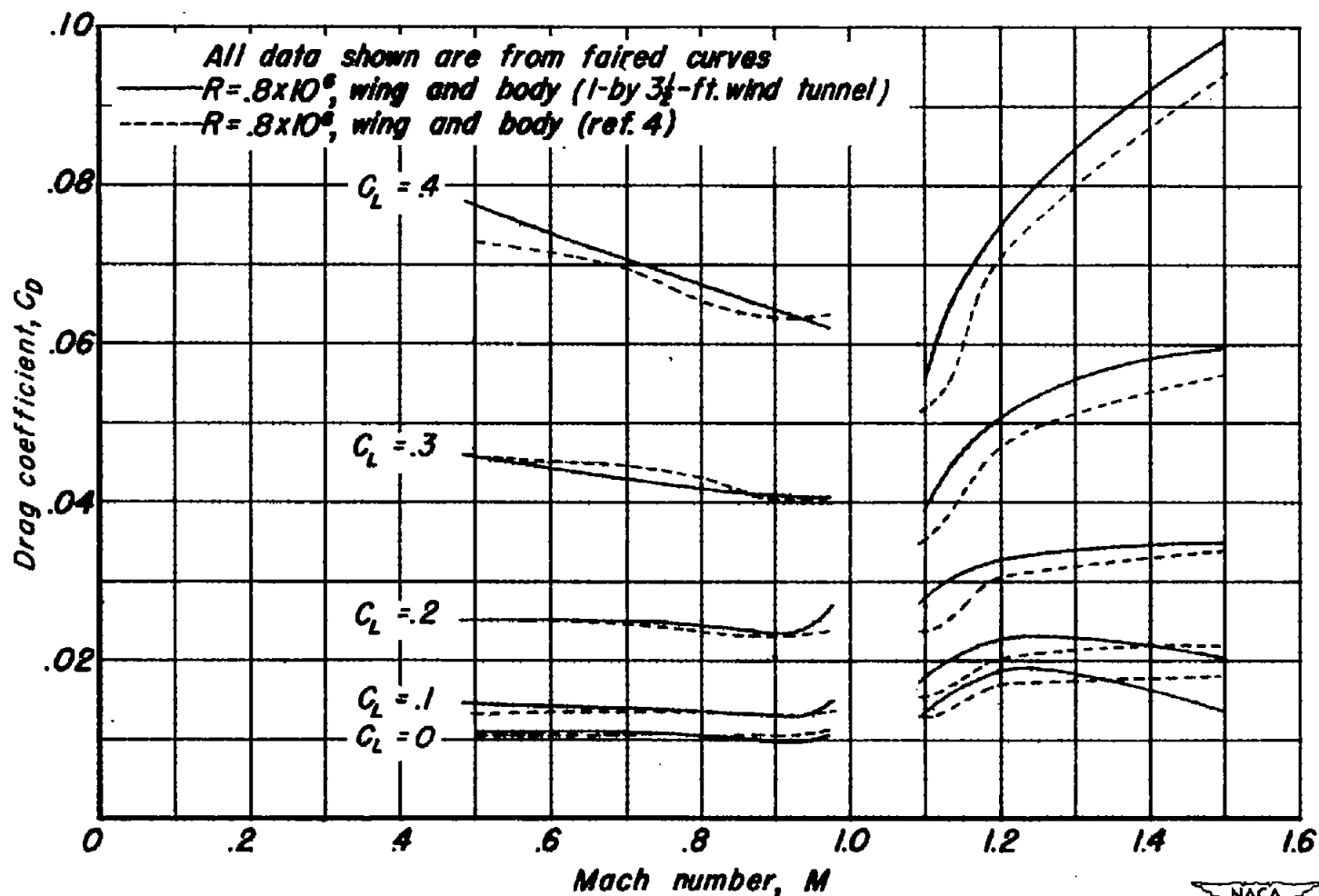


Figure 7.— The variation of drag coefficient with Mach number at constant lift coefficient.



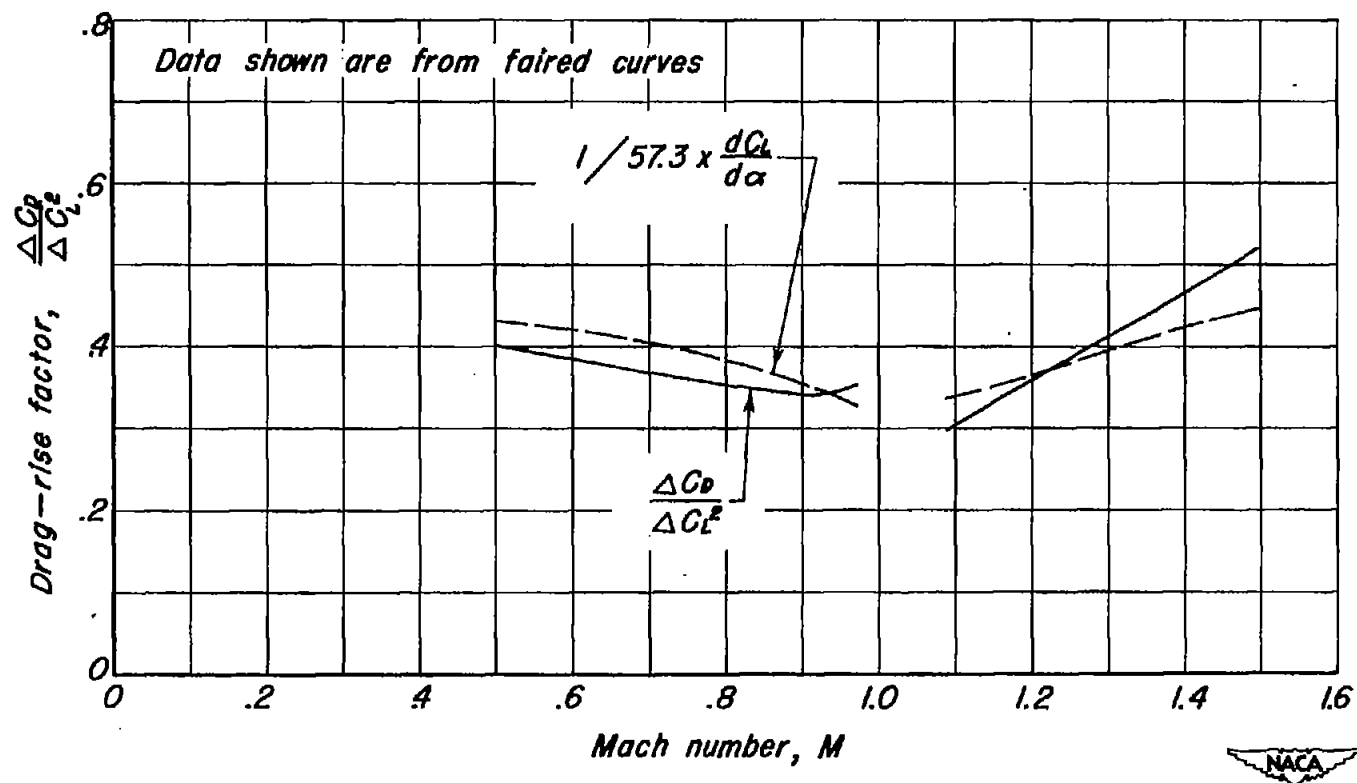


Figure 8.—The variation of the drag-rise factor with Mach number.

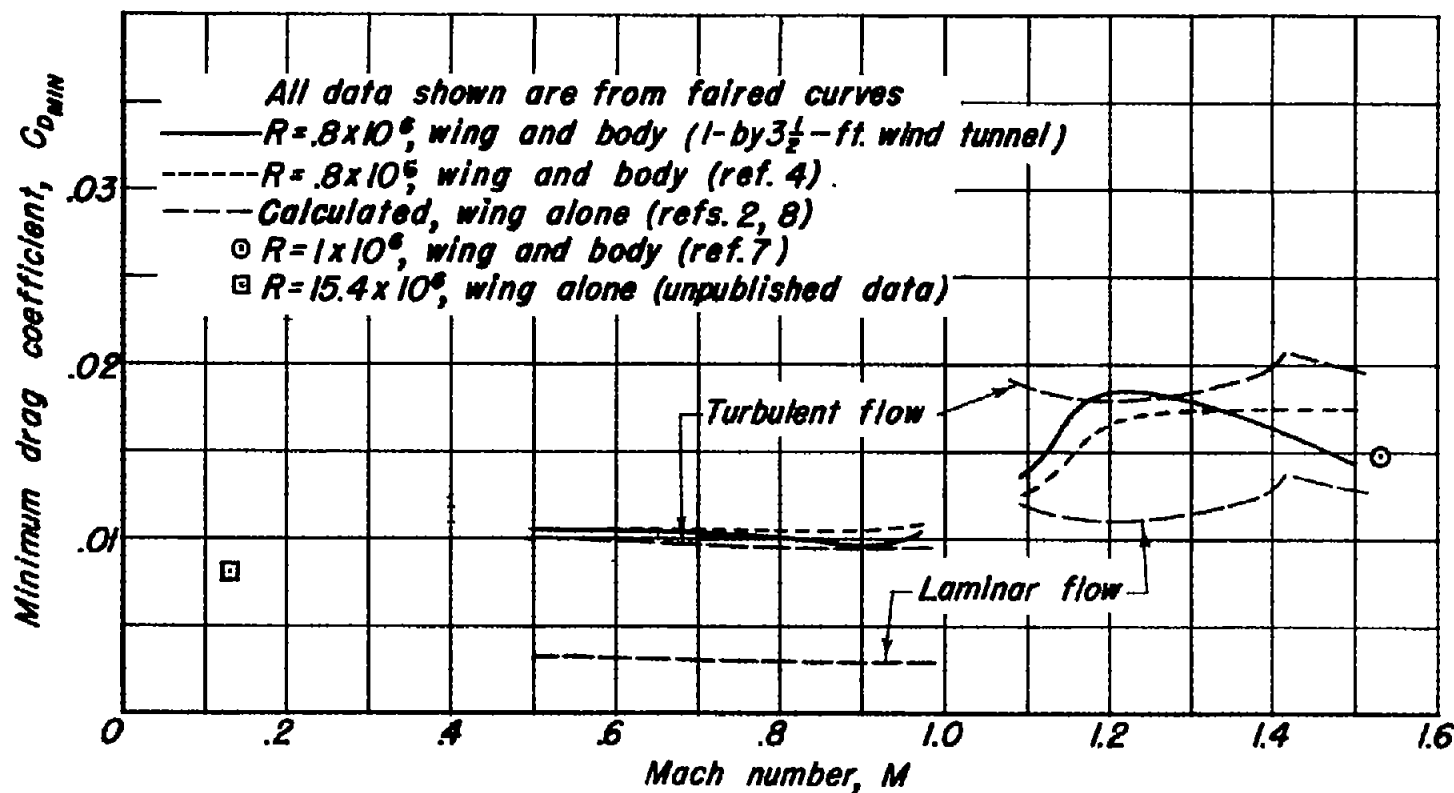


Figure 9.— The variation of minimum drag coefficient with Mach number.



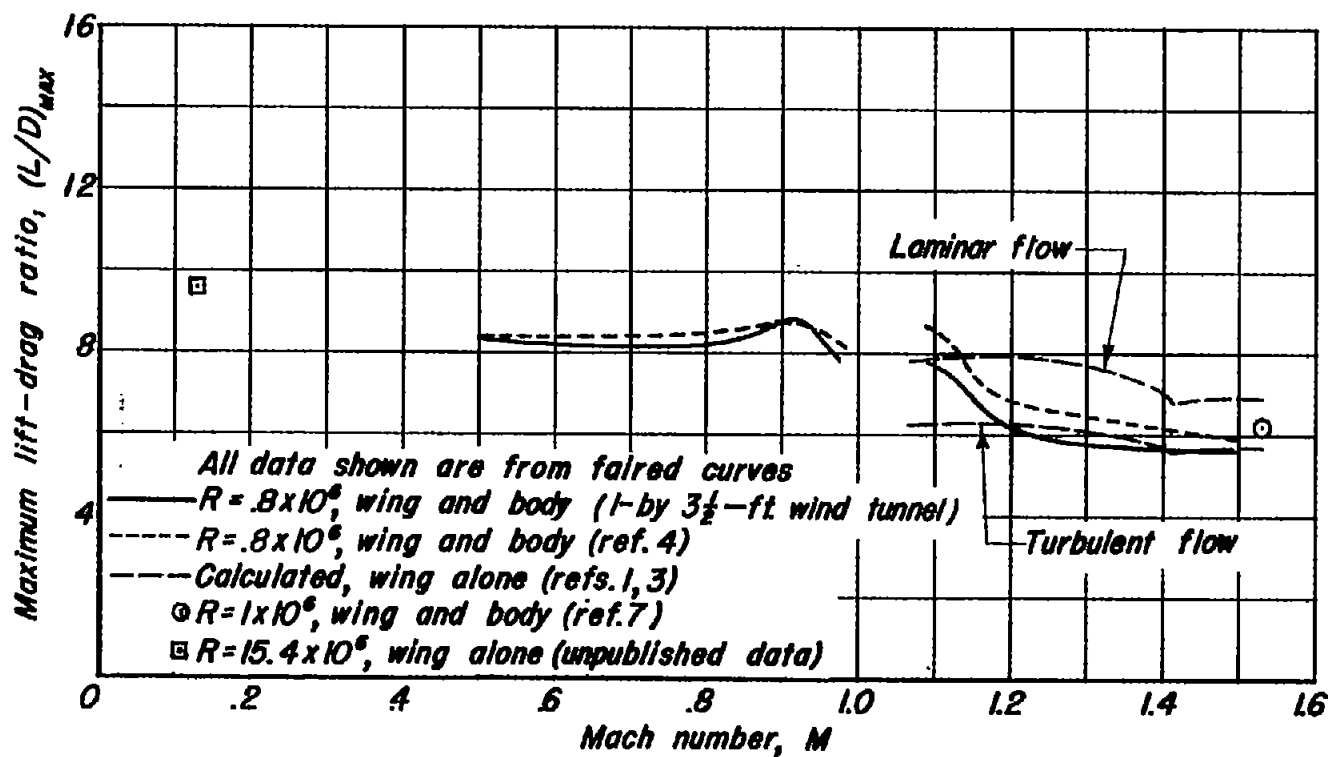


Figure 10.— The variation of maximum lift-drag ratio with Mach number.



529/c

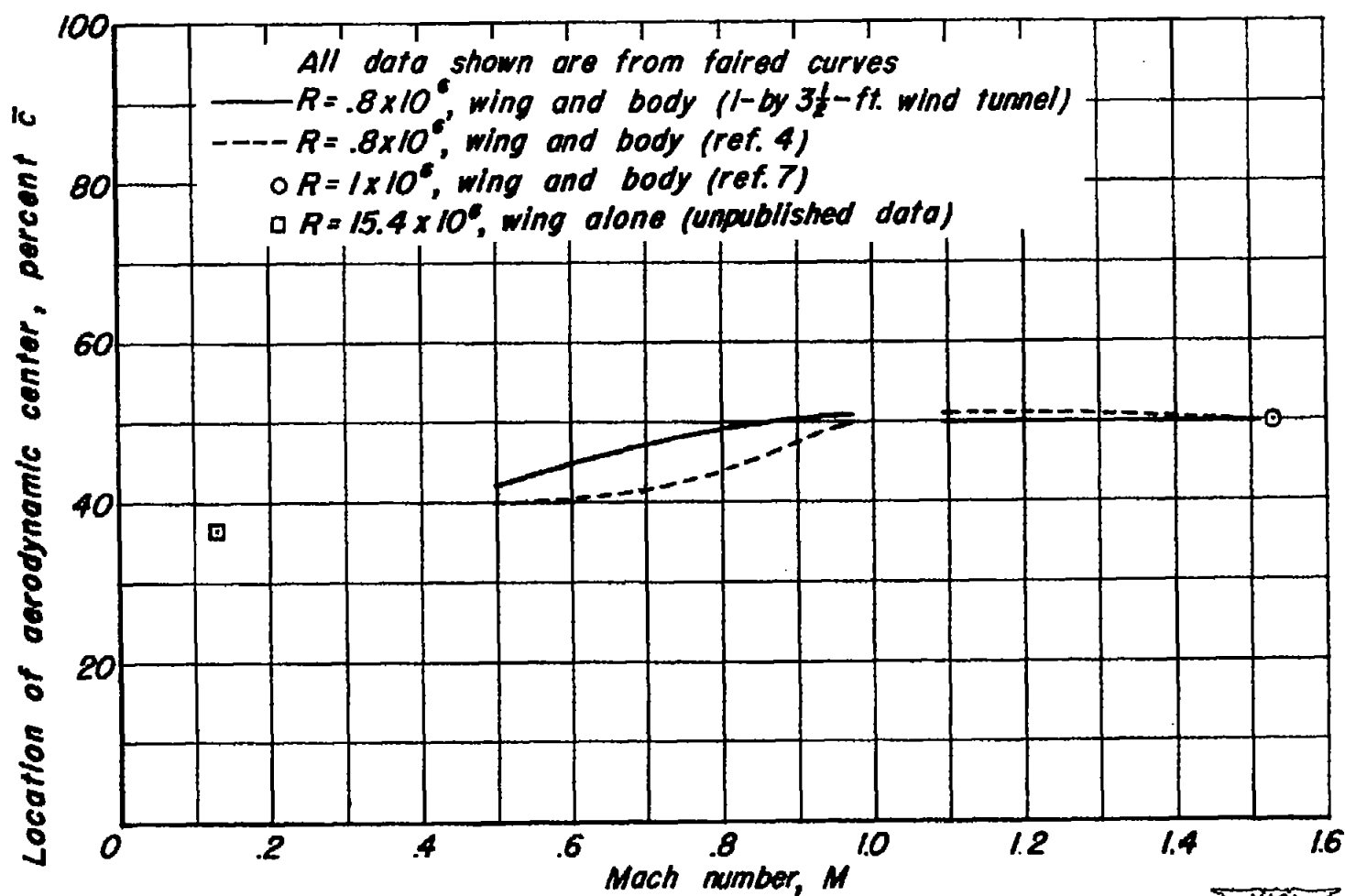
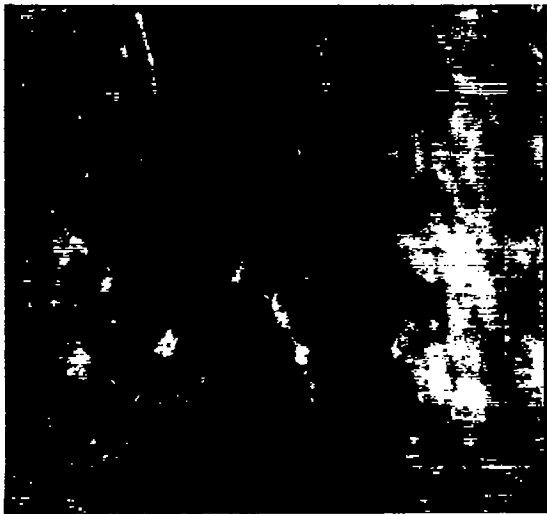
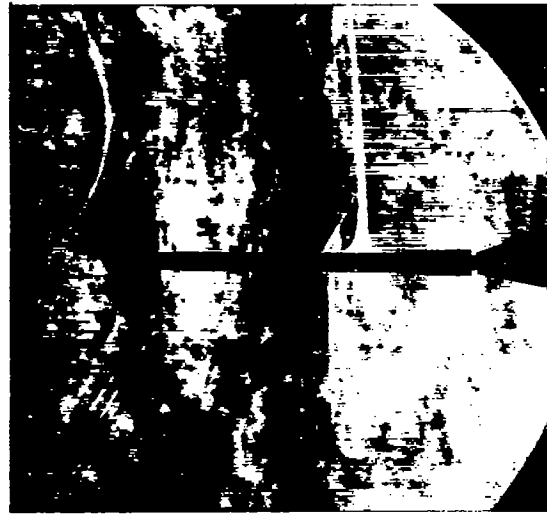


Figure 11.—The variation of aerodynamic center with Mach number.





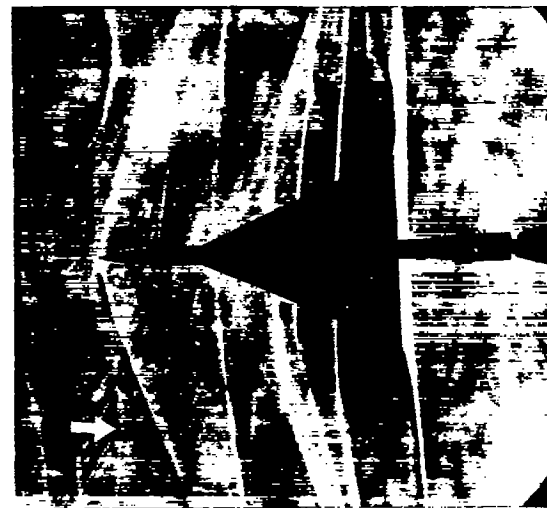
(a) Air stream off.



(b)  $M = 0.95$ , side view.



(c)  $M = 1.09$ , side view.



(d)  $M = 1.09$ , plan view.

NACA  
A-12840

Figure 12.— Typical schlieren photographs of the side and plan views of the model at several Mach numbers.





(e)  $M = 1.12$ , side view.



(f)  $M = 1.12$ , plan view.



(g)  $M = 1.29$ , side view.



(h)  $M = 1.29$ , plan view.

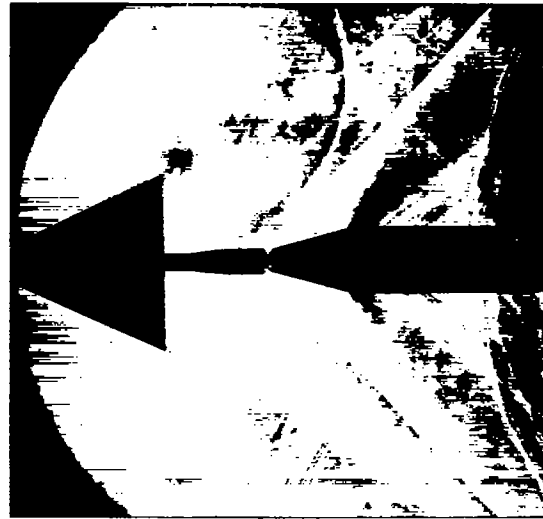
NACA  
A-12839







(i)  $M = 1.49$ , side view.



(j)  $M = 1.49$ , plan view.

NACA  
A-12841

NASA Technical Library



3 1176 01434 4650